JTTEE5 17:796–804
DOI: 10.1007/s11666-008-9266-1
1059-9630/$19.00 © ASM International

Peer Reviewed

Fast Regime Fluidized Bed Machining (FR-FBM) of Thermally Sprayed Coatings

Massimiliano Barletta, Gianluca Rubino, Giovanni Bolelli, and Luca Lusvarghi

(*Submitted June 9, 2008; in revised form September 15, 2008*)

Finishing of thermally sprayed metallic, ceramic, and cermet coatings is required to meet tolerances and requirements on surface roughness in most industrial applications. Conventional machining is a costly and time-consuming process, and is difficult to automate. Therefore, this study investigates and develops a new technique highly amenable for automation: fast regime—fluidized bed machining (FR-FBM). Atmospheric plasma sprayed TiO_2, Cr_2O_3, and HVOF-sprayed WC-17%Co and Tribaloy-800 coatings, deposited on AISI 1040 steel substrates, were subjected to FR-FBM treatment. The effects of the leading operational parameters, namely, abrasive size, jet pressure, and processing time, were evaluated on all coatings by using a two/three-levels full factorial design of experiments. The FR-FBM treated surfaces were observed by FE-SEM and their surface finishing was evaluated by contact profilometry. Significant improvements in surface finishing of all the machined thermally sprayed coatings can always be detected, with FR-FBM being able to guarantee the precision and to ensure the closest geometrical tolerances.

Keywords automatic machining, atmospheric plasma spraying, fluidized bed, HVOF

1. Introduction

The conception of highly stressed components requires a fine assessment of materials, design, and manufacturing techniques. Whenever components withstanding dynamic solicitations have to be developed, their surface plays a crucial role, because damages often start in the outermost layers at notches, pores, fatigue slip steps, and inclusions (Ref 1). In this respect, the various techniques for surface treatment are assuming a remarkable interest in several industrial fields. Among them, the application of surface overlay coatings by thermal spray techniques is spreading over a wide range of applications, often including the manufacturing of high performance components (Ref 2). Nonetheless, reprocessing of the as-deposited thermally sprayed coatings is often necessary to meet surface finishing requirements and, above all, to ensure the closest geometrical tolerances (Ref 3). Nowadays, conventional reprocessing techniques are still costly and time consuming and are rather troublesome to automate (Ref 2, 3). Besides, conventional machining solutions are often manual, thus displaying poor or, at least, unstable results and strict dependency on the capability of skilled technicians (Ref 3, 4).

This is, therefore, the context in which the present study moves to analyze the possibility to apply fast regime—fluidized bed machininig (FR-FBM) for surface finishing of a wide range of thermally sprayed coatings by atmospheric plasma sprayed (APS) and HVOF. In particular, the influence of FR-FBM operational parameters on the resultant surface finishes was thoroughly investigated according to a design of experiments (DOE)-assisted experimental schedule. Furthermore, the morphological characteristics of the finished surfaces were examined by combined usage of SEM and contact-mode profilometry. Finally, variations in tribological properties before and after FR-FBM were evaluated by pin-on-disk tests. In the light of experimental findings, FR-FBM was found to significantly improve the finishing of thermally sprayed coatings, hence guaranteeing superior visual appearance, high machining accuracy, and good precision.

2. Experimental

2.1 Material

Four different thermally sprayed coatings were selected for the present test, namely, atmospheric plasma sprayed TiO_2 (deposition parameters in Ref 4, thickness 168 ± 16 μm), APS Cr_2O_3 (parameters in Ref 5, thickness 330 ± 21 μm), HVOF-sprayed WC-17%Co (thickness

This article is an invited paper selected from presentations at the 2008 International Thermal Spray Conference and has been expanded from the original presentation. It is simultaneously published in *Thermal Spray Crossing Borders, Proceedings of the 2008 International Thermal Spray Conference*, Maastricht, The Netherlands, June 2-4, 2008, Basil R. Marple, Margaret M. Hyland, Yuk-Chiu Lau, Chang-Jiu Li, Rogerio S. Lima, and Ghislain Montavon, Ed., ASM International, Materials Park, OH, 2008.

Massimiliano Barletta and **Gianluca Rubino**, Dipartimento di Meccanica ed Aeronautica, 'La Sapienza' Università di Roma, Via Eudossiana, 18, 00184 Rome, Italy; and **Giovanni Bolelli** and **Luca Lusvarghi**, Dipartimento di Ingegneria dei Materiali e dell'Ambiente, Università degli Studi di Modena e Reggio Emilia, Via Vignolese, 905, 41100 Modena, Italy. Contact e-mail: Barletta@ing.uniroma2.it.

230 ± 15 μm) (Ref 6), and Tribaloy-800 (thickness 402 ± 14 μm) (Ref 7), deposited on AISI 1040 steel substrates. Slabs 10 × 10 × 5 mm^3 were subjected to FR-FBM treatment.

Unsieved alumina powders (Smyris Abrasivi, Como, Italy) were used as abrasive media for finishing purposes. Abrasive sizes were 46, 80, and 180 mesh size (MS). The different sized powders were all characterized by a rather angular shape factor of about 0.67, this being the guarantee of the presence on them of a large number of 'self-sharpening cutting tools' (i.e., the sharp edges and the tips of the angular abrasive particle).

2.2 Apparatus

FR-FBM was used for easy-to-automate finishing of the thermally sprayed coatings. The description of FR-FBM system is detailed elsewhere (Ref 8-10).

Figure 1 shows a sketch of the system, which consists of an air feeding system (mostly, a blower), an air plenum chamber to ensure the proper air feeding to the fluidization column and its distribution across the column, a porous plate distributor, which allows the fluidization air to pass through while it retains the powders to be fluidized, a fluidized bed column in which the fluidization takes place, a couple of cyclones, a static or rotating sample holder, and, then, controls, tubes, valves, and all the necessary fittings.

Purified air is forced through the porous plate distributor (sintered bronze, 8 mm thick, average porosity of 70 μm) and acts to suspend the abrasive powders (typically, Al_2O_3) preloaded inside the fluidized bed column (40 × 40 × 1200 mm^3, AISI 304). The substrate to be finished is held inside the fluidization column by using a shaft (3 mm diameter, AISI 304). A direct current electrical motor is used to rotate the sample inside the fluidized abrasives, hence changing the impact conditions between the abrasives and the surface to be finished and ensuring fresh abrasive is repeatedly delivered toward the target.

During FR-FBM, abrasives and fines produced because of the heavy machining conditions tend to raise up through the fluidized bed column and they are progressively elutriated from the top of the column as a result of the fluidization in fast regime. To prevent the rapid emptying of the fluidized bed column and ensure the continuity of FR-FBM, a cyclone is located downstream the fluidized bed column to collect the elutriated abrasives and resupply them at the bottom of the column itself. A second cyclone is, then, used to recover the fines produced during the heavy machining, thus avoiding their unsafe dispersion to the environment.

2.3 Procedure

The effects of leading FBM operational parameters, namely, abrasive size, jet pressure, and processing time, on the surface finish of the thermally sprayed coatings were evaluated using a full factorial DOE. Table 1 summarizes the experimental schedule.

Table 1 Design of experiments

Mesh size (MS), μ/in	Abrasives diameter, μm	Pressure, Pa	Time, min
46	~354	4×10^5	2
80	177	4×10^5	2
180	~88	4×10^5	2
46	~354	4×10^5	5
80	177	4×10^5	5
180	~88	4×10^5	5
46	~354	7×10^5	2
80	177	7×10^5	2
180	~88	7×10^5	2
46	~354	7×10^5	5
80	177	7×10^5	5
180	~88	7×10^5	5

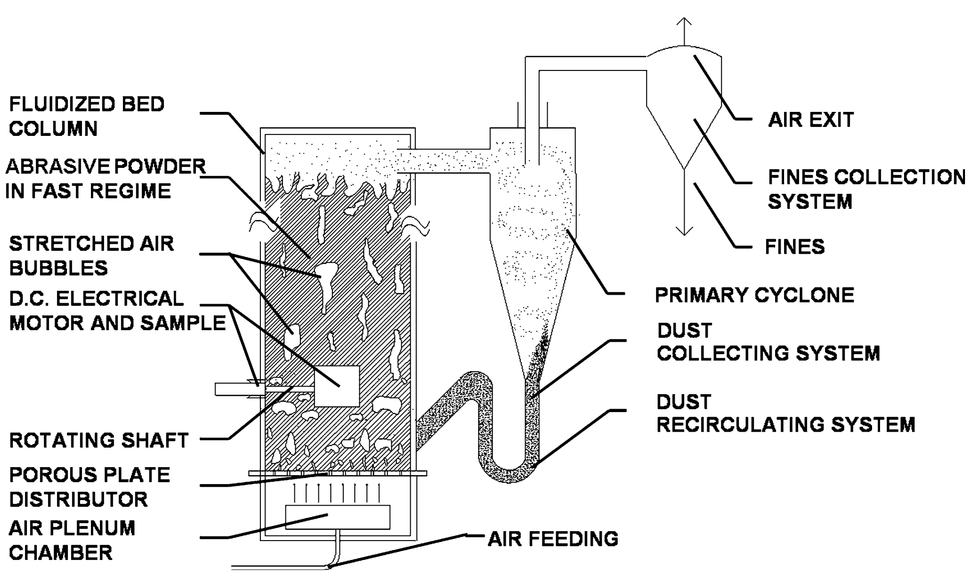

Fig. 1 The FR-FBM system

Mass loss after FR-FBM was calculated by using a Sartorious BP 211-D weighing instrument (0.01 mg resolution). Each workpiece was measured several times, and if the difference between the two following measurements failed to agree within 0.5 mg, the measurements were repeated again until agreement within this range was attained in successive determinations. The change in thickness was also carefully evaluated by using a Mitutoyo Absolute Digimatic Micrometers Series 227 (±1 μm resolution). A map of nine measurements equally spaced over the machined coatings were performed. This way, the evenness of the coating removal process, and thus the suitability of FR-FBM in obtaining tight tolerances, was carefully checked.

Surface roughness measurements were carried out using a contact-mode profilometer (Taylor-Hobson CLI 2000). TalyMap software release 3.1 was employed to work out the amplitude, spacing, and hybrid roughness parameters. For such purpose, wide enough areas of 4 × 4 and 7 × 7 mm^2 with a lateral resolution of 1 μm along the measurement direction and, respectively, of 4 and 100 μm along the perpendicular direction were measured. Finally, a Field Emission Scanning Electron Microscope (FE-SEM Leo Supra 35) was employed to obtain high resolution images of the machined surfaces at various levels of magnification.

3. Results and Discussion

The interactions between the fluidized abrasives and the surface to be finished were first analyzed by evaluating the mass loss and the material removal of the thermally sprayed coatings varying the FR-FBM operational parameters. In particular, machining conditions, which made use of abrasives MS 46, were first considered as it was supposed that the biggest abrasives produced the massive effects and the largest dimensional changes in the machined substrates.

Figures 2(a) and (b) reports the mass loss and the material removal, respectively. Both mass loss and material removal were found to increase drastically whenever higher jet pressure was set. Furthermore, if their trends are looked into, it is possible to note how very large reductions in the samples mass and in their thickness are induced by an increase in jet pressure, while slighter reduction was induced by an increase in the machining time. However, no strict relationship between the mass loss and the reduction in the coating thickness can be supposed, as the mass loss is very much influenced by the embedding phenomena of abrasive debris inside the outermost layers of the thermally sprayed coating as a result of the heavy machining conditions. This way, the measurement of the mass variation is altered by the presence of abrasive residuals into the machined surface, as the evidence of SEM image in Fig. 3 shows and in agreement with what is reported in the pertinent literature for similar process conditions (Ref 8-10).

It is also worth mentioning how the variance of coating thickness is very low (Fig. 2b) although measurements

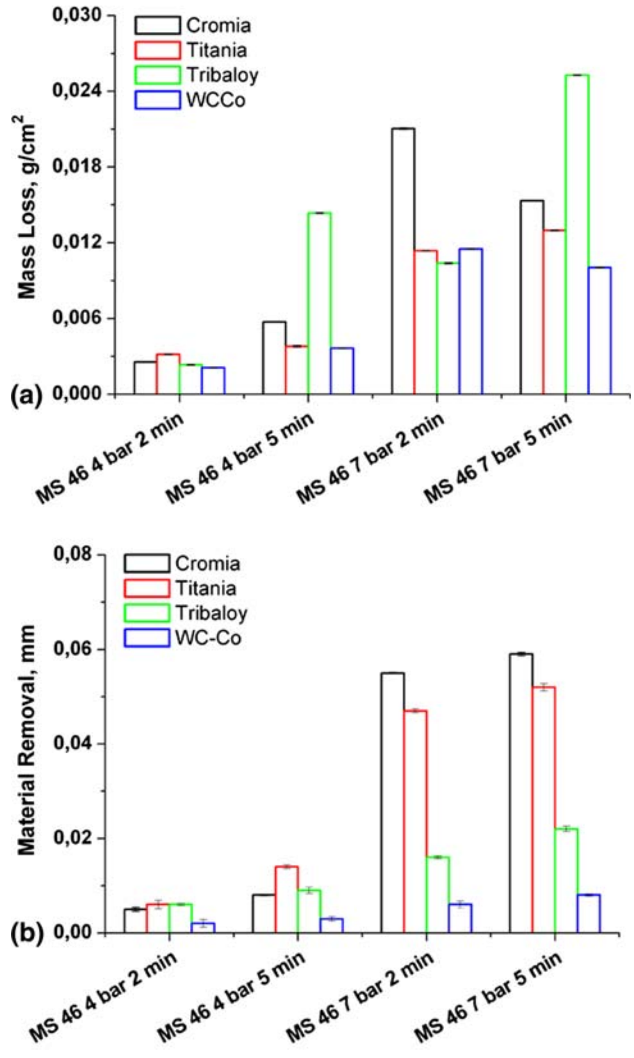

Fig. 2 (a) Mass loss and (b) material removal of thermally sprayed coatings after FR-FBM

were taken on nine different locations equally spaced over the treated samples. This suggests that FR-FBM can be a very promising technique to evenly machine thick and hard coatings and, thus, to ensure the closest geometrical tolerances. Further test on more complicated sample geometries would however be required to ascertain the evenness of the FR-FBM treatment and its capability to respect the dimensional tolerances.

Noticeable differences in the variation of samples mass and thickness characterize the investigated coating materials. Indeed, the different coating materials behave differently as a result of their specific hardness and toughness (Ref 4-7). WC-Co-based coatings, which present high hardness coupled with satisfactory toughness (Ref 5, 6), tend to be very difficult to machine, thus leading to minimum material removal during FR-FBM. Indeed, this favorable combination of material properties makes these coatings highly resistant to particle erosion (Ref 11, 12), a process similar to that occurring in FR-FBM. However,

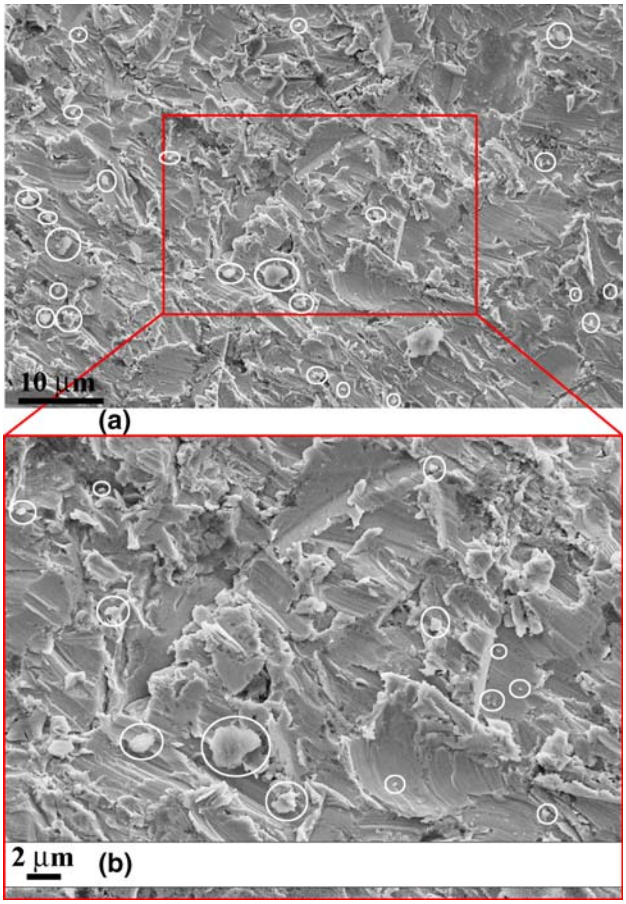

Fig. 3 (a) Abrasive splinters clung onto a TiO_2 coating after FR-FBM and (b) Higher magnification of the embedded abrasive particles

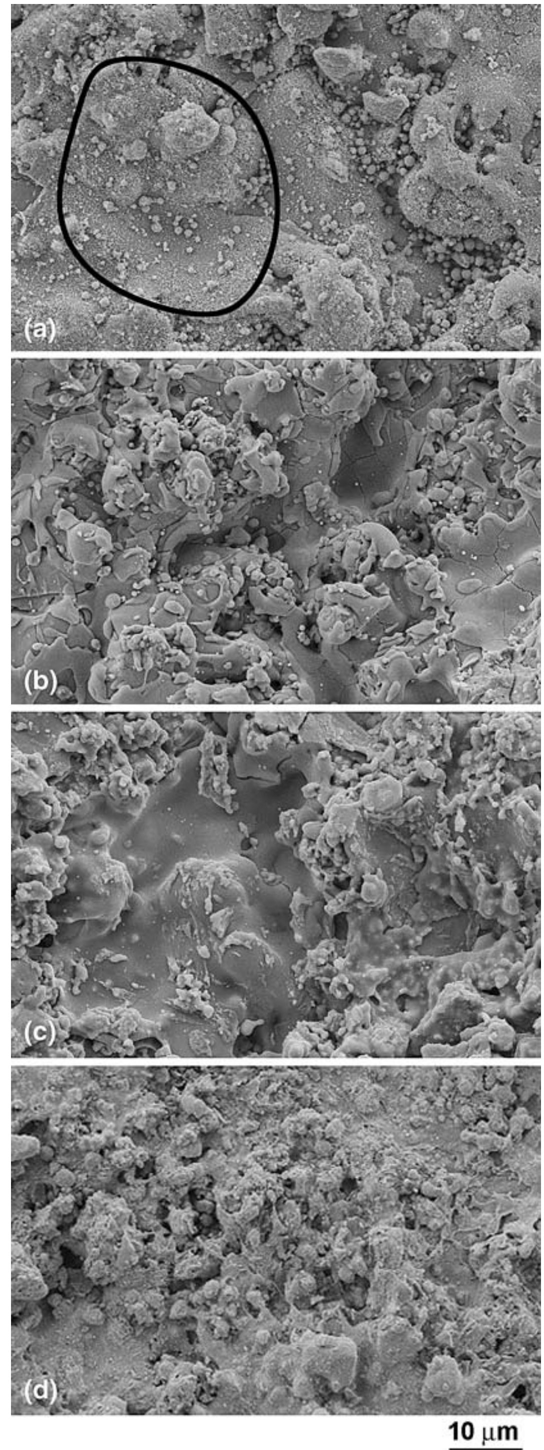

Fig. 4 SEM images of the thermally sprayed coating before FR-FBM (MS 80, jet pressure 7 bar, and machining time 5 min): (a) Cr_2O_3 as-deposited (the *circle* indicates a clearly recognizable lamella); (b) TiO_2 as-deposited; (c) Tribaloy-800 as-deposited; and (d) WC-17%Co as-deposited

WC-Co coatings are rather sensitive to the changes in FR-FBM operational parameters. In fact, material removal can increase up to four times setting the jet pressure and the machining time at their maximum.

SEM micrographs (Fig. 4 and 5) reveal that material is removed from the as-deposited WC-Co coating surface (which exhibits a rough morphology, Fig. 4(d), due to the incomplete flattening of particles impinging in a semisolid state, as shown in Ref 13, 14 by a combination of ductile grooving and carbide fracture (Fig. 6), probably caused by erodent particles impinging at low or high (close to 90°) angles, respectively, consistently with erosion mechanisms described in Ref 11, 12.

Conversely, APS-Cr_2O_3 coatings do exhibit very large amount of material removal at any time the jet pressure is set at 7 bar. APS-Cr_2O_3 is the hardest among the present coatings, but it is also rather brittle (i.e., poor toughness) (Ref 5): this compromises its resistance to the more energetic impacts of the fluidized abrasives, thus determining severe mass loss via brittle fracture phenomena, a well-known erosive wear mechanism for APS ceramics (Ref 15). Indeed, on the FR-FBM-processed surface of Cr_2O_3, the gently curved morphology of sprayed lamellae is still well recognizable (compare the circled area in Fig. 5a to the lamella shown in Fig. 4a), indicating that material was removed by cracks running preferentially along interlamellar boundaries (Fig. 5a, arrows indicate

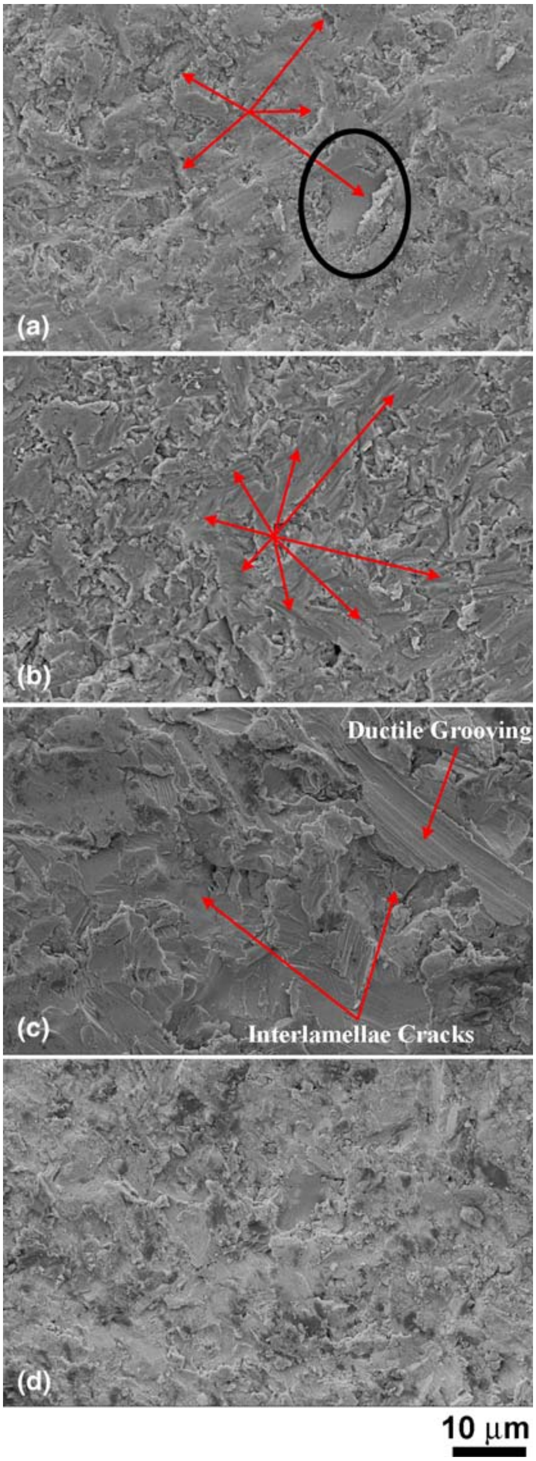

Fig. 5 SEM images of the thermally sprayed coatings after FR-FBM (MS 80, jet pressure 7 bar, and machining time 5 min): (a) Cr_2O_3 finished (*arrows*: interlamellae cracks; *circle*: a portion of a lamella uncovered by detachment of the above layers); (b) TiO_2 finished (*arrow*: ductile grooving); (c) Tribaloy-800 finished, and (d) WC-CO 17% finished

some recognizable cracks). Indeed, such clear tendency to anisotropic crack propagation in this coating was formerly proven by indentation tests (Ref 5); moreover, an

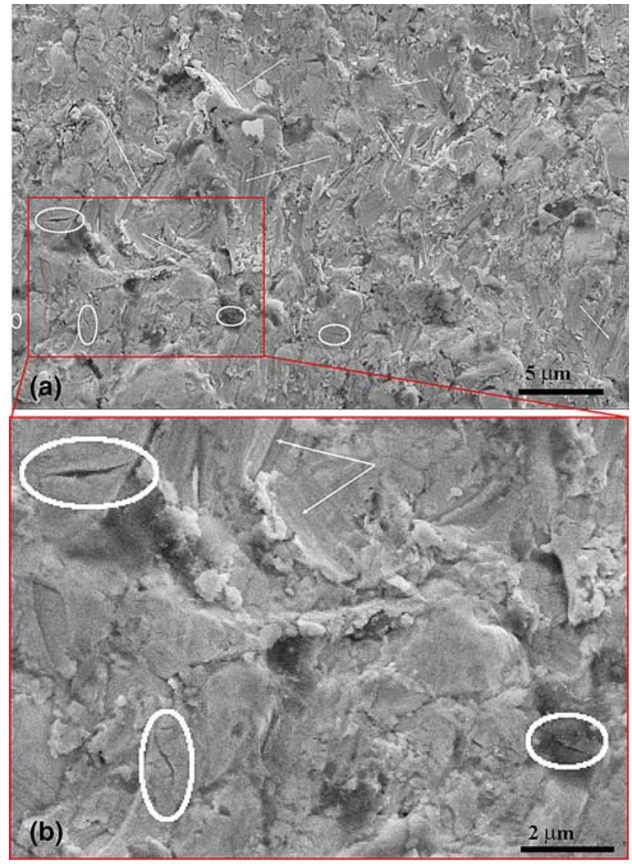

Fig. 6 (a) SEM image of ductile grooving (i.e., *white arrows*) and carbide grains fracture (i.e., *white circle*) onto WC-Co coating after FR-FBM and (b) higher magnification of ductile grooving and carbide grains fracture

analogous wear mechanism was noted in dry particle abrasion tests (Ref 5). However, Cr_2O_3-based coatings also present the largest difference in behavior when machined at high and low jet pressures. In fact, at low jet pressure, they are less sensitive to the machining action of the abrasives as a result of their high hardness. At high jet pressure, the prominent effect of their rather poor toughness can increase the material removal rate by more than one order of magnitude.

TiO_2-based coatings behave differently. Their hardness ($HV_{0.1} = (10.31 \pm 1.11)$ GPa, Ref 4) is lower than that of Cr_2O_3-based coatings ($HV_{0.1} = (12.52 \pm 1.26)$ GPa, Ref 5), but their toughness is higher. Indeed, even though the quantitative reliability of indentation fracture toughness measurements on APS ceramics was criticized in Ref 4 by some of the authors, a useful qualitative ranking can be obtained: APS-Cr_2O_3 exhibited K_{Ic} to be (1.67 ± 0.67) MPa $m^{1/2}$, while for APS-TiO_2, using the data collected in Ref 4, it is computed to be (2.11 ± 0.41) MPa $m^{1/2}$, which confirms its better toughness. Therefore, TiO_2-based coatings present the highest material removal after FR-FBM at low pressure as a result of the very low hardness. At high pressure, TiO_2-based coatings keep on showing rather large material removal, but their good toughness prevents them to behave worse than the Cr_2O_3-based coatings. Indeed, the material removal mechanism of APS-TiO_2 is significantly different from that of Cr_2O_3. Indeed, ductile grooves appear in the former (Fig. 5b), witnessing the occurrence of microscale plastic deformation (microcutting and/or microploughing), which is in strict agreement with the report by Liu et al. (Ref 16) on abrasive machining of thermally sprayed coatings. They indicated that material removal by plastic grooving occurs below a critical depth-of-cut value, while brittle fracture prevails above that value. The critical depth-of-cut is given by the relation:

$$d_C = \beta \frac{E/HV}{(HV/K_{IC})^2}$$

where β is a constant and E, HV, and K_{IC} are elastic modulus, Vickers hardness, and toughness, respectively. Using the values listed above, $E = 129$ GPa for TiO_2 (Ref 4) and $E = 132$ GPa for Cr_2O_3 (Ref 17), the ratio between the critical depth-of-cut on Cr_2O_3 and that on TiO_2 is estimated to be 0.36. Thus, it is clearly explained why, under the same conditions, the former coating is much more prone to undergo brittle fracture.

Tribaloy coatings are softer but tougher. For this reason, they display intermediate machining behavior between the WC-Co-based coatings, which undergo lower surface modification due to superior hardness, and the Ti and Cr oxides, which undergo deeper alteration. In particular, remarkable grooving, together with limited interlamellar failure, is noted (Fig. 5c).

The evaluation of surface finishing of thermally sprayed coatings was performed by evaluating the variations in roughness parameters before and after FR-FBM. Figure 7 reports the trend of the average roughness R_a. In as-deposited condition, the various coatings possess different roughness values, since the particles clearly possess different behaviors, both in-flight and upon impact, due to different thermophysical material properties, different particle size distributions, and different spray conditions (including torch type and parameter setting). Useful indications are achieved by evaluating the relative improvement in roughness values after FR-FBM.

The data are in good agreement with that mentioned previously about the mass loss and material removal of the different thermally sprayed coatings after FR-FBM. In particular, TiO_2-based coatings present the most significant variations in R_a. Abrasives MS 46 and 80 lead to improvements of three to four times in R_a, which approach values as low as 1.6-1.7 μm. Indeed, remarkable plastic grooving helps cutting and removing the large surface asperities existing in as-deposited condition due to the lamellar structure, thus making the surface smoother and more homogeneous. Analogously, tribaloy coatings display very large improvements in R_a, with values reduced by about 250%, when the largest abrasives and high operating pressure are employed, since, under these conditions, a very efficient surface machining by plastic grooving is also obtained. Instead, under less energetic machining conditions (MS 180), the mechanical properties of the tribaloy coatings are high enough to make them

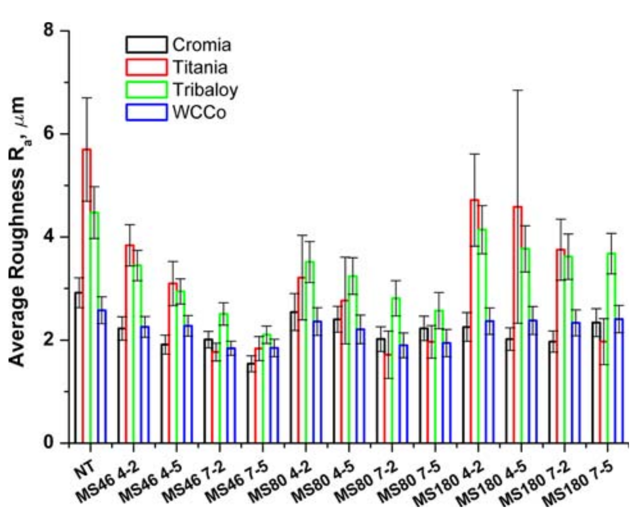

Fig. 7 Average roughness R_a of thermally sprayed coatings after FR-FBM (Note: NT = nontreated coatings)

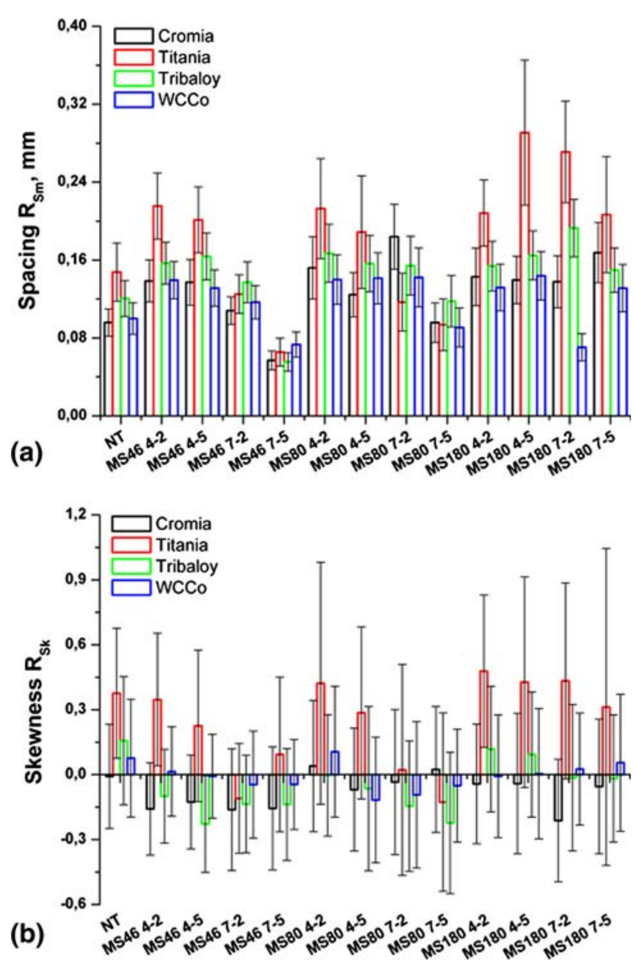

Fig. 8 (a) Spacing R_{Sm} and (b) skewness R_{sk} of thermally sprayed coatings after FR-FBM (Note: NT = non-treated coatings)

almost insensitive to the FR-FBM. In fact, in that operating condition, the improvements in R_a are very small, whatever the setting of the jet pressure and of the machining time. Cr_2O_3- and WC-Co-based coatings display the lowest variations in R_a, with improvements in surface finish in the range of 30-40%, when the more energetic machining conditions (MS 46 or 80, higher jet pressure) are set. Such result can be interpreted as follows. Concerning WC-17%Co, its high hardness and the toughness reduce, to a larger extent, the machining capability of the FR-FBM. Concerning Cr_2O_3, under less intense machining conditions, the high hardness can also reduce the finishing effects, consistently with the low material loss; instead, under more energetic conditions, the onset of brittle fracture wear prevents substantial roughness improvements, because new lamellae are continuously being uncovered, as described earlier.

Figure 7 also reveals that R_a approaches very similar values for all the thermally sprayed coatings, whenever effective machining conditions are set. In fact, abrasives MS 46 or 80 joined with a jet pressure of 7 bar and a machining time of 2 or 5 min lead to R_a in the range of 1.6-2.4 μm, apart from the starting roughness and the coatings material. Accordingly, a hypothesis of a sort of asymptotic finishing conditions, typical of the FR-FBM technique, can be definitely formulated. This result is in agreement with what was found in a previous work of one of the authors, which usefully identifies an asymptotic finishing condition for two different aluminum alloys submitted to a fluidized bed of abrasives in bubble regime (Ref 18). However, these observations reveal that some improvement can still be expected for the more ductile coatings (APS TiO_2 and HVOF tribaloy), while little improvements are expected on HVOF WC-17%Co and on APS Cr_2O_3, the latter being possibly the most unsuitable coating for this kind of machining process.

Figures 8(a) and (b) reports spacing R_{Sm} and skewness R_{sk} of the thermally sprayed coatings before and after FR-FBM. R_{Sm} shows the lowest values at any time abrasives MS 46 and 80 are joined with high jet pressure.

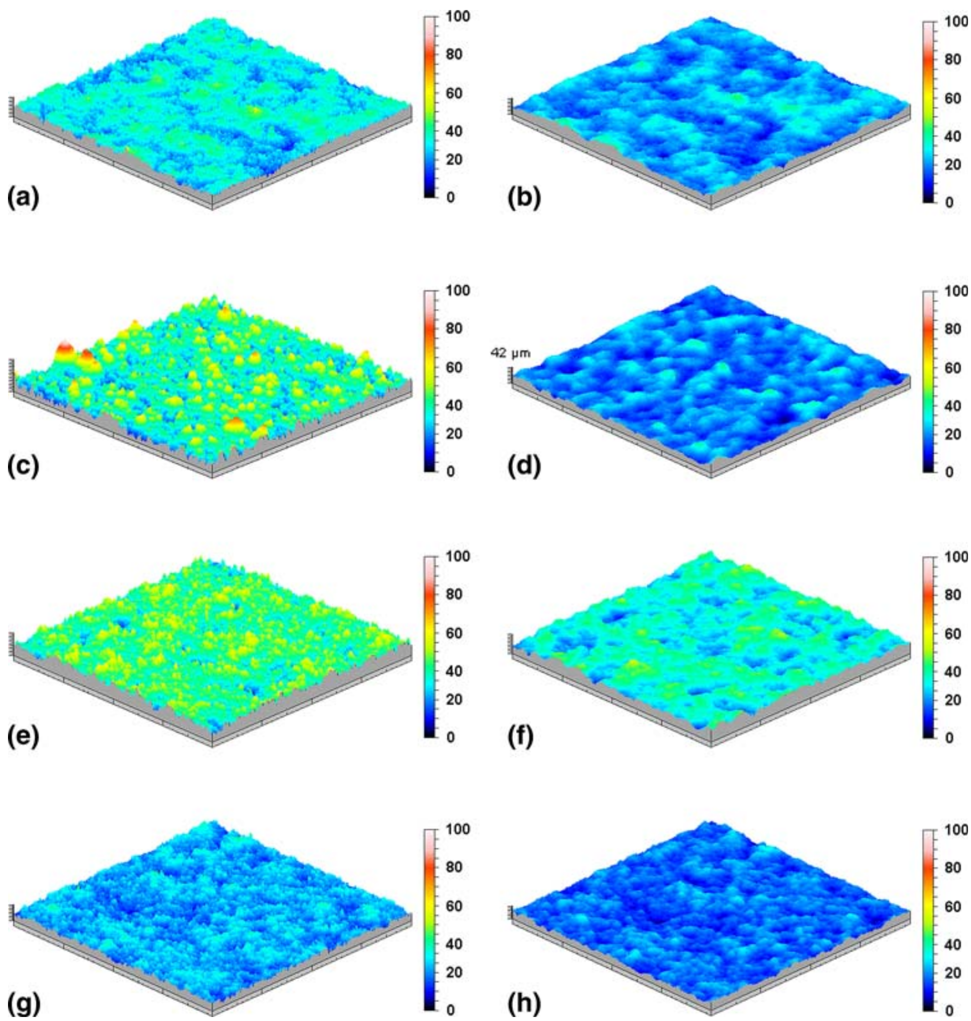

Fig. 9 3D maps of thermally sprayed coatings before and after FR-FBM (MS 80, jet pressure 7 bar, machining time 5 min): (a) Cr_2O_3 as-deposited; (b) Cr_2O_3 finished; (c) TiO_2 as-deposited; (d) TiO_2 finished; (e) Tribaloy-800 as-deposited; (f) Tribaloy-800 finished; (g) WC-CO17% as-deposited; (h) WC-CO17% finished

Peer Reviewed

This result is ascribable to the presence of widespread microcraters all over the finished surface due to the high energetic impacts of the fluidized abrasives projected at high speed toward the surface to be finished. This way, the finished surface acquires a typical texture due to the characteristics of the FR-FBM.

This can be also the reason why all the materials finished in such FR-FBM conditions (MS 46 or 80, jet pressure of 7 bar, machining time of 2 or 5 min) approach nearly the same value of the R_a apart from the starting surface morphology.

The trend of skewness reveals further crucial aspects about the FR-FBM of the thermally sprayed coatings.

R_{Sk} turns negative at any time sufficiently energetic machining is performed. R_{Sk} negative means surface profile with prevalently upward material, that is, rather smooth surface. As seen, the result of the repeated actions of the abrasives all over the surface can result in a significant change in the overall morphology of the as-deposited thermally sprayed coatings even at a large scale. The achievable variations are displayed in the 3D maps reported in Fig. 9, which report an overview of the status of the thermally sprayed coatings before and after FR-FBM. As can be clearly appreciated, a significant smoothening of the surface finish can always be claimed whatever the coatings material, with an apparent flattening of the coarser morphological features, which initially spread all over the starting surface morphology, and the corresponding establishment of a quite smooth surface finish.

4. Conclusions

The present study deals with an application of FR-FBM for finishing of different thermally sprayed coatings. From the examination of the experimental findings, the following conclusions can be drawn:

(i) Machining capability of FR-FBM depends on the mechanical properties of the thermally sprayed coatings and, in particular, on the hardness at low jet pressure and on the toughness at high jet pressure. The best surface finish improvements are achieved when ductile grooving mechanisms occur. Therefore, harder and tougher materials are troublesome to machine. Analogously, excessively brittle materials, prone to undergo brittle fracture, are difficult to process.

(ii) Significant improvement in surface finish can be detected for TiO_2 and Tribaloy-800 coatings, which are know to present moderate hardness and sufficient toughness. Indeed, machining takes place by ductile grooving. In such cases, improvement in average roughness from 250 to 400% can be claimed.

(iii) The surface finishing of the thermally sprayed coatings, matter of the present investigation, always improves, thus approaching an average roughness of from 1.6 to 2.4 μm independently of the starting morphology and the material properties.

(iv) FR-FBM is a first step toward the automatization of the finishing process of thermally sprayed coatings, which, at the present, are only hand-machined by skilled technicians with recursive time- and cost-consuming procedures.

To conclude, FR-FBM can be a valid and easy-to-automate alternative to the handmade finishing techniques of the thermally sprayed coatings. Further research and optimization is certainly needed to optimize processing conditions and surface finishing of the tested coatings. In particular, future analyses will regard the application of FR-FBM to the finishing of complex-shaped components.

Acknowledgments

The authors wish to thank Mr. Ceccarelli (Università di Roma 'Tor Vergata') for the setup of the apparatus. They also wish to acknowledge Mr. Bassani and Mr. Pighetti (Università di Modena e Reggio Emilia) for the preparation of the samples.

References

1. C.M. Verpoort and C. Gerdes, *Shot Peening, Theory and Applications*, IITT International, Gorunay-Sur-Marne, France, 1989, p 11-70
2. T. Bernecki, *Handbook of Thermal Spray Technology*, J.R. Davis, Ed., 14-35, 2004 (Materials Park, OH), ASM International, 2004
3. Z.W. Zhong, Z.F. Peng, and N. Liu, Surface Roughness Characterization of Thermally Sprayed and Precision Machined WC–Co and Alloy-625 Coatings, *Mater. Charact.*, 2007, **58**, p 997-1005
4. G. Bolelli, V. Cannillo, L. Lusvarghi, F. Pighetti Mantini, E. Gualtieri, and C. Menozzi, An FIB Study of Sharp Indentation Testing on Plasma-Sprayed TiO_2, *Mater. Lett.*, doi:10.1016/j.matlet.2007.09.022
5. G. Bolelli, V. Cannillo, L. Lusvarghi, and T. Manfredini, Wear Behaviour of Thermally Sprayed Ceramic Oxide Coatings, *Wear*, 2006, **261**, p 1298-1315
6. G. Bolelli, V. Cannillo, L. Lusvarghi, and S. Riccò, Mechanical and Tribological Properties of Electrolytic Hard Chrome and HVOF-Sprayed Coatings, *Surf. Coat. Tech.*, 2006, **200**, p 2995-3009
7. G. Bolelli, V. Cannillo, L. Lusvarghi, M. Montorsi, F. Pighetti Mantini, and M Barletta, Microstructural and Tribological Comparison of HVOF-Sprayed and Post-treated M-Mo-Cr-Si (M = Co, Ni) Alloy Coatings, *Wear*, 2007, **263**, p 1397-1416
8. M. Barletta and V. Tagliaferri, Development of an Abrasive Jet Machining System Assisted by Two Fluidized Beds for Internal Polishing of Circular Tubes, *Int. J. Mach. Tool Manuf.*, 2006, **46**(3-4), p 271-283
9. M. Barletta, S. Guarino, G. Rubino, and V. Tagliaferri, Progress in Fluidized Bed Assisted Abrasive Jet Machining (FB-AJM): Internal Polishing of Aluminium Tubes, *Int. J. Mach. Tool Manuf.*, 2007, **47**(3-4), p 483-495
10. M. Barletta, D. Ceccarelli, S. Guarino, and V. Tagliaferri, Fluidized Bed Assisted Abrasive Jet Machining (FB-AJM): Precision Internal Finishing of Inconel 718 Components, *J. Manuf. Sci. E-T ASME*, 2007, **129**, p 1-15
11. H.M. Hawthorne, B. Arsenault, J.P. Immarigeon, J.G. Legoux, and V.R. Parameswaran, Comparison of Slurry and Dry Erosion Behaviour of Some HVOF Thermal Sprayed Coatings, *Wear*, 1999, **225-229**, p 825-834

12. P. Kulu, I. Hussainova, and R. Veinthal, Solid Particle Erosion of Thermal Sprayed Coatings, *Wear*, 2005, **258**, p 488-496
13. S. Kamnis, S. Gu, T.J. Lu, and C. Chen, Computational Simulation of Thermally Sprayed WC–Co Powder, *Comput. Mater. Sci.*, 2008, **43**(4), p 1172-1182
14. W. Trompetter, M. Hyland, D. McGrouther, P. Munroe, and A. Markwitz, Effect of the Substrate Hardness on Particle Morphology in High Velocity Thermal Spray Coatings, *J. Therm. Spray Technol.*, 2006, **15**, p 663-669
15. R. Westergård, N. Axén, U. Wiklund, and S. Hogmark, An Evaluation of Plasma Sprayed Ceramic Coatings by Erosion, Abrasion and Bend Testing, *Wear*, 2000, **246**, p 12-19
16. X. Liu, B. Zhang, and Z. Deng, Grinding of Nanostructured Ceramic Coatings: Surface Observations and Material Removal Mechanisms, *Int. J. Mach. Tool Manuf.*, 2002, **42**, p 1665-1676
17. G. Bolelli, L. Lusvarghi, T. Manfredini, F Pighetti Mantini, R Polini, E Turunen, T Varis, and S-P Hannula, Comparison Between Plasma- and HVOF-Sprayed Ceramic Coatings. Part I: Microstructure and Mechanical Properties, *Int. J. Surf. Sci. Eng.*, 2007, **1**(1), p 38-61
18. M. Barletta, A New Technology in Surface Finishing: Fluidized Bed Machining (FBM) of Aluminium Alloys, *J. Mater. Process. Tech.*, 2006, **173**, p 157-165